

A numerical approach for the bifurcation analysis of nonsmooth delay equations

Joseph Páez Chávez^{a,c}, Zhi Zhang^b, Yang Liu^{b,*}

^a*Center for Applied Dynamical Systems and Computational Methods (CADSCOM), Faculty of Natural Sciences and Mathematics, Escuela Superior Politécnica del Litoral, P.O. Box 09-01-5863, Guayaquil, Ecuador*

^b*College of Engineering Mathematics and Physical Sciences, University of Exeter, Harrison Building, North Park Road, Exeter EX4 4QF, UK*

^c*Center for Dynamics, Department of Mathematics, TU Dresden, D-01062 Dresden, Germany*

Abstract

Mathematical models based on nonsmooth dynamical systems with delay are widely used to understand complex phenomena, specially in biology, mechanics and control. Due to the infinite-dimensional nature of dynamical systems with delay, analytical studies of such models are difficult and can provide in general only limited results, in particular when some kind of nonsmooth phenomenon is involved, such as impacts, switches, impulses, etc. Consequently, numerical approximations are fundamental to gain both a quantitative and qualitative insight into the model dynamics, for instance via numerical continuation techniques. Due to the complex analytical framework and numerical challenges related to delayed nonsmooth systems, there exists so far no dedicated software package to carry out numerical continuation for such type of models. In the present work, we propose an approximation scheme for nonsmooth dynamical systems with delay that allows a numerical bifurcation analysis via continuation (path-following) methods, using existing numerical packages, such as COCO (Dankowicz and Schilder). The approximation scheme is based on the well-known fact that delay differential equations can be approximated via large systems of ODEs. The effectiveness of the proposed numerical scheme is tested on a case study given by a periodically forced impact oscillator driven by a time-delayed feedback controller.

Keywords: Delay differential equation; Piecewise-smooth dynamical system; Large system of ODEs; Bifurcation; Numerical continuation

1. Introduction

Delay differential equations (DDEs) are widely used in physical, mechanical, and biological systems to simulate the time delay phenomena caused by human observer [1], feedback control [2], actuation [3], and communication [4]. With the introduction of time delay in differential equations, the model can be more accurate for predicting the real system. For example, the mathematical model describing tumour growth under a treatment by chemotherapy incorporates time delay relating to the conversion from resting to hunting cells [5]. A simple delay mathematical model [6] can describe the dynamics of AIDS-related cancers with treatment of HIV and chemotherapy. The state-dependent time delay inherently exists in the downhole drilling process [7]. On the other hand, time delay is sometimes artificially introduced to the system for control purposes. For example, constant maturation time delay, pulse pesticide input, and pulse harvesting prey may have obvious effects on the predator-prey model with stage-structure for pests [8]. Pyragas [9] proposed to use the famous delayed self-controlling feedback for chaos control, which does not require a priori analytical knowledge of the system dynamics and are applicable to experiment. However, the available general-purpose computational tools for the numerical treatment of smooth DDEs are rather

*Corresponding author. Tel: +44(0)1392-724654, e-mail: y.liu2@exeter.ac.uk.

Email addresses: jpaez@espol.edu.ec (Joseph Páez Chávez), zz326@exeter.ac.uk (Zhi Zhang), y.liu2@exeter.ac.uk (Yang Liu)

limited, and almost nonexistent for piecewise-smooth DDEs, specially for numerical bifurcation analysis. The main reason is due to the analytical and numerical challenges owing to the infinite-dimensional nature of dynamical systems with delay, in combination with the presence of nonsmooth phenomena. Therefore, while a number of software packages have been developed for numerical continuation in smooth DDEs (e.g. DDE-BIFTOOL [10, 11], PDDE-CONT [12] and Knut [13]), no software package of this kind exists for the path-following analysis of piecewise-smooth DDEs, which is one of the main motivations of the present work.

One way to numerical study the dynamical response of a DDE is via the approximation of the original equation by a high-dimensional system of ordinary differential equations. For example, Repin [14] proposed a system of ODEs to approximate a DDE through a first-order approximation of the original solution, currently referred to as the *chain method*. Later on, Gyori and Turi [15] proved the uniform convergence of this method for a DDE in an infinite interval. In [16], Westdal and Lehn proposed the time optimal control by approximating the linear time invariant differential-difference system. Hess [17] used this method to approximate the linear differential equation with a large time delay. Further improvements of the numerical approach proposed in [14] were introduced in the work by Banks [18]. This numerical framework was later employed by Lipták *et al.* [19] to study delayed chemical reaction networks.

Piecewise-smooth dynamical systems have received considerable attention in the past, mainly due to their crucial role played in understanding complex nonsmooth phenomena. For instance, in the study of piecewise linear suspension bridge model [20], the model of a DC-DC buck converter [21], and the recurrent dynamics of human gait system [22]. For the bifurcation analysis of this type of systems, a number of continuation tools have been developed in the past, for instance, TC-HAT [23], SlideCont [24] and the multi-segment continuation capability included in COCO [25]. However, when time delay is introduced, there is no continuation software available to carry out bifurcation studies via path-following routines. In the past, however, a solid numerical framework has been proposed for this task (see e.g. [26–28]), but the related codes are not yet available in a user friendly and general-purpose form.

Therefore, the main goal of the present work is to propose an approximation method for nonsmooth DDEs, which enables the numerical bifurcation analysis of the system dynamics via existing and well-established numerical continuation packages, such as COCO [25]. The proposed numerical approach is based on the *chain method* outlined above, in combination with a second-order approximation scheme of the original DDE by considering a finite sequence of Taylor expansions as proposed in [29]. In this way, a piecewise-smooth dynamical system with (constant) delay can be approximated by a piecewise-smooth system of ODEs of large dimension, which then allows the study of the resulting model in the framework of hybrid dynamical systems, following the ideas of [28] and [23].

The proposed numerical scheme will be applied in the present work to study a periodically excited oscillator with soft impacts [30, 31], driven by a time-delayed feedback controller. Many engineering applications experiencing repeated collisions at their mechanical parts can be represented using a soft-impact model as the one considered here, where the discontinuity boundary is neither motion- nor time-dependent but fixed at a constant. One of the main questions in such mechanical scenarios is to identify parameter values that allows the user to drive the system from impacting to non-impacting system responses and viceversa, in a controllable and reliable manner. In our numerical investigation, we will employ the proposed approximation scheme to tackle the question outlined above via numerical continuation. Specifically, we will try to identify grazing phenomena defining the boundary between impacting and non-impacting dynamical behavior, and hence determine precise control parameter values to achieve this purpose via the classical time-delayed feedback controller [9].

The rest of the paper is organized as follows. Section 2 presents the basic mathematical framework for the study of dynamical systems with delay, as well as a detailed development of the numerical approach to approximate their solutions via systems of ODEs of large dimension. In Section 3, the physical and mathematical description of the impact oscillator is presented, together with its formulation as a hybrid dynamical system and numerical approximation considering the time-delay feedback controller. After that the system is analyzed numerically via the continuation software COCO in Section 4. This part also includes some preliminary numerical tests regarding the approximation properties of the proposed numerical scheme. Finally, the main conclusions of the present work are given in Section 5.

2. Approximation of delay differential equations via large systems of ODEs

As mentioned before, the main goal of the present work is to develop a numerical approach in order to analyze piecewise-smooth DDEs via path-following (continuation) methods. Numerical continuation is a well-established technique that permits an in-depth analysis of a system dynamics, under parameter variations. In particular, it allows tracing certain invariant sets (such as equilibria, periodic orbits, homoclinic orbits, etc.) as selected system parameters vary, usually via a predictor-corrector approach [32]. For ODEs there is a variety of software packages that are widely used for numerical continuation in such class of models, for example AUTO [33], CONTENT [34] and MATCONT [35], among many others. On the other hand, software tools for piecewise-smooth systems are much less abundant, being SLIDECONT [24], TC-HAT [23] and COCO [25] essentially the only available in the field. Similarly, path-following software for (smooth) DDEs have received relatively little attention in the literature, with the packages DDE-BIFTOOL [10] and PDDE-CONT [12] being the most widely used tools for such type of models.

To the best of our knowledge, there is no software package able to perform numerical continuation for DDEs considering nonsmooth phenomena, such as impacts, switches, impulses, etc. Numerical continuation of periodic solutions in piecewise-smooth DDEs has been carried out by Barton [28], where the author combines the mathematical framework designed for hybrid dynamical systems [23] with a multi-point boundary-value problem that is then embedded in a numerical continuation setting, whose applicability is illustrated in four different examples. From this work, however, no software packages or codes have been made available for general applications. Another approach for dealing with piecewise-smooth DDEs consists in substituting Heaviside and sign functions by a tanh function with certain calibrating parameters to adjust the desired degree of approximation to the original functions [12, 26, 27]. After the replacements have been made, the original system is turned into a smooth DDE for which any of the continuation tools mentioned in the previous paragraph can be applied. This approach, however, presents some limitations, especially when the considered orbit possesses a nontrivial *solution signature* [23, 28]. In addition, this technique cannot be applied when the DDE considers impulsive perturbations, and also it does not allow the study of dynamical phenomena inherent to nonsmooth systems, such as grazing and sliding events. Therefore, in the present work we will propose a different approach, consisting in approximating a DDE via large systems of ODEs, in combination with the mathematical formulation for hybrid dynamical systems, which then allows the application of any of the software tools mentioned above, designed for nonsmooth dynamical systems.

2.1. Basic mathematical setup

Delay differential equations can be considered as dynamical systems of infinite dimension, where the present state depends also on values in the past [36–38]. Such systems are usually defined over the Banach space of continuous functions $C([- \tau_{\max}, 0], \mathbb{R}^d)$, equipped with the supremum norm, where $\tau_{\max} > 0$ represents the largest delay, $d \geq 1$. For some $t_0 \in \mathbb{R}$ and $\sigma > 0$, suppose that $x : [t_0 - \tau_{\max}, t_0 + \sigma] \rightarrow \mathbb{R}^d$ is a continuous mapping. Then, for any $t \in [t_0, t_0 + \sigma]$, we define $x_t(\theta) := x(t + \theta)$, $\theta \in [-\tau_{\max}, 0]$. Under this setting, we say that [39]

$$\dot{x} = F(t, x_t), \tag{2.1}$$

is a retarded functional differential equation (RFDE), where $F : \Omega \rightarrow \mathbb{R}^d$ is a given function, with Ω being an open subset of $\mathbb{R} \times C([- \tau_{\max}, 0], \mathbb{R}^d)$. A function $x \in C([t_0 - \tau_{\max}, t_0 + \sigma], \mathbb{R}^d)$ is called a solution to (2.1) if $(t, x_t) \in \Omega$ and x satisfies (2.1) for all $t \in [t_0, t_0 + \sigma]$. The solution to (2.1) can be made unique [36] if we assume that F is continuous and locally Lipschitz with respect to its second argument and impose the initial condition $x_{t_0} = \phi$, for some fixed $\phi \in C([- \tau_{\max}, 0], \mathbb{R}^d)$.

An important feature of the RFDE (2.1) is that of *smoothing* [39], i.e., an increase in the regularity of the solution x as the time t grows. Specifically, it can be shown [40] that if F is of class C^k , $k \geq 1$, and $I := [t_0, \sigma_{\max})$ stands for the maximum interval of existence for the solution x , then x is of class C^q on $[t_0 + q\tau_{\max}, \sigma_{\max})$ for $q = 0, 1, \dots, k$, provided $t_0 + q\tau_{\max}$ does not exceed σ_{\max} . In particular, one has that periodic solutions are as smooth as the operator F [41], a property that can be exploited for the numerical approximation of the solution of the RFDE (2.1) that will be introduced in the next section.

2.2. Numerical approach

In this work, we will be interested in analyzing a particular type of retarded functional differential equation (see (2.1)), namely

$$\dot{x}(t) = f(t, x(t), x(t - \tau_d)), \quad (2.2)$$

which represents a system of delay differential equations (DDEs) with constant delay $\tau_d > 0$, where $f : \mathbb{R} \times \mathbb{R}^d \times \mathbb{R}^d \rightarrow \mathbb{R}^d$ is a sufficiently smooth function. As we mentioned previously, the type of equations considered here can be seen as dynamical systems with an infinite-dimensional phase space, due to which analytical studies of such systems are generally difficult and require careful mathematical treatment. The situation becomes even more complicated when some kind of nonsmooth phenomenon is involved, such as impacts, switches, impulses, etc., as we will see later. Consequently, numerical approximations are fundamental to gain both a quantitative and qualitative insight into the model dynamics.

A preliminary approach to reduce the infinite-dimensional problem to one of finite dimension is via a Taylor expansion [42]:

$$x(t - \tau_d) = \sum_{k=0}^M x^{(k)}(t) \frac{(-\tau_d)^k}{k!} + \mathcal{O}\left(\tau_d^{M+1}\right), \quad (2.3)$$

which can then be inserted into (2.2) (neglecting the \mathcal{O} -terms), hence obtaining a system of ordinary differential equations of high order, see for example [43, 44] for practical applications of this technique. This is by all means an analytically valid approach, however, it suffers from certain limitations. For instance, the power series expansion (2.3) provides good approximations depending on the size of the delay τ_d and how many terms are used in the expansion (which depends on M). Therefore, this approach restricts the size of the delay and also may require the solution to be many times differentiable, which is not always the case. The main idea, however, can be slightly modified in order to overcome the aforementioned limitations, by considering a finite sequence of Taylor expansions as follows [29].

For the sake of simplicity, let us assume that the solution x of (2.2) is as smooth as required for our discussion, which can be achieved via the smoothing property outlined in the previous section. Take $N \in \mathbb{N}$ sufficiently large and define the grid points $t_i := i\frac{\tau_d}{N}$, $i = 0, \dots, N$. Furthermore, define $u_i(t) := x(t - t_i)$ for all $t \geq 0$, $i = 0, \dots, N$. In this setting, we obtain via Taylor expansion that

$$u_{i-1}(t) = x\left(t - \left(t_i - \frac{\tau_d}{N}\right)\right) = u_i\left(t + \frac{\tau_d}{N}\right) = \sum_{k=0}^M \frac{1}{k!} u_i^{(k)}(t) \left(\frac{\tau_d}{N}\right)^k + \mathcal{O}\left(\left(\frac{\tau_d}{N}\right)^{M+1}\right), \quad \text{and} \quad (2.4)$$

$$\dot{u}_0(t) = f(t, u_0(t), u_N(t)), \quad (2.5)$$

for all $t \geq 0$, $i = 1, \dots, N$, $M \geq 1$. After neglecting the \mathcal{O} -terms, we obtain from (2.4) a system of dN differential equations of order M . As is well known, the resulting set of equations can then be written as a first-order system of ODEs, in such a way that we obtain $d(NM + 1)$ ordinary differential equations (from (2.4) and (2.5)) in order to approximate the solution of the DDE (2.2). If $M = 1$ is chosen, the approach outlined above reduces itself to the well-known *chain method*, which results in the following system of $d(N + 1)$ ODEs:

$$\begin{cases} \dot{u}_0(t) = f(t, u_0(t), u_N(t)), & t \geq 0, \\ \dot{u}_i(t) = \frac{N}{\tau_d} (u_{i-1}(t) - u_i(t)), & t \geq 0, \quad i = 1, \dots, N, \\ u_i(0) = \phi\left(-i\frac{\tau_d}{N}\right), & i = 0, \dots, N, \end{cases} \quad (2.6)$$

where $\phi \in C([-\tau_{\max}, 0], \mathbb{R}^d)$ is a suitably chosen initial function at $t_0 = 0$ (i.e. $x_{t_0} = x_0 = \phi$). This approximating system was developed and studied since mid 1960s, see for example the works by Krasovskii [45], Repin [14] and Westdal [16]. In particular, it has been shown that the solution of (2.6) converges uniformly to the solution of the original DDE (2.2) as $N \rightarrow \infty$, provided the initial function ϕ is suitably chosen [14]. Further results regarding convergence have been derived in the past, see for instance the

studies by Gyori et al. [15, 46], Banks [18] and Demidenko [47], as well as recent applications in practical problems [19, 48]. In the present work, we will apply a second-order approximation of the DDE (2.2) based on the general scheme shown in (2.4) and (2.5), which takes the following form

$$\begin{cases} \dot{u}_0(t) = f(t, u_0(t), u_N(t)), & t \geq 0, \\ \dot{u}_i(t) = w_i(t), & t \geq 0, \quad i = 1, \dots, N, \\ \dot{w}_i(t) = \frac{2N^2}{\tau_d^2} \left(u_{i-1}(t) - u_i(t) - \frac{\tau_d}{N} w_i(t) \right), & t \geq 0, \quad i = 1, \dots, N, \end{cases} \quad (2.7)$$

where w_i , $i = 1, \dots, N$, represent auxiliary functions introduced to write the approximating system as a set of $d(2N + 1)$ first-order scalar ODEs.

2.3. Mathematical framework for piecewise-smooth DDEs

A simple example of a piecewise-smooth DDE, considering two vector fields and an impulsive perturbation [49], is given by

$$\begin{cases} \dot{x}(t) = f_1(t, x(t), x(t - \tau_d)), & h(x(t), x(t - \tau_d)) > 0, \\ \dot{x}(t) = f_2(t, x(t), x(t - \tau_d)), & h(x(t), x(t - \tau_d)) < 0, \\ x(t^+) = g(x(t^-)), & h(x(t), x(t - \tau_d)) = 0, \end{cases} \quad (2.8)$$

where $f_{1,2} : \mathbb{R} \times \mathbb{R}^d \times \mathbb{R}^d \rightarrow \mathbb{R}^d$, $h : \mathbb{R}^d \times \mathbb{R}^d \rightarrow \mathbb{R}$ and $g : \mathbb{R}^d \rightarrow \mathbb{R}^d$ are sufficiently smooth functions. Model (2.8) belongs to the class of *hybrid dynamical systems* [50], which are characterized by a continuous evolution interrupted by discrete events, hence producing a piecewise-continuous flow. This type of systems appears typically in applications dealing with switches, impacts, stick-slip phenomena, etc. A classical example is that of an elastic ball bouncing on a rigid surface. A continuous evolution of the ball position is produced under action of the gravity. However, a discontinuous transition occurs every time the ball touches the rigid surface. At this moment, the ball experiences an “instantaneous” reversal of its direction of motion, and the magnitude of the outgoing velocity is usually assumed to be smaller than that of the velocity right before the impact (Newton’s restitution law). The general framework to model this type of dynamical systems consists in dividing the state space into disjoint subregions associated to a particular operation mode of the system, described by a certain smooth vector field (f_1 and f_2 in system (2.8)). A transition to a different mode of operation takes place whenever a system trajectory reaches the boundary of the corresponding subregion. The boundaries are often defined as the zero-set of smooth scalar functions (referred to as *event functions*, given by the function h in system (2.8)), which normally describe physical instantaneous events, such as impacts, switches, transitions from stick to slip motion, etc., as mentioned earlier. Once a transition has been detected, the vector field describing the system behavior is changed according to the governing laws of the system, and the initial point of the next system trajectory is defined by a certain *reset function*, represented by the mapping g in (2.8). In the example of the bouncing ball, the reset function would be given in terms of the described restitution law that reverses and reduces the magnitude of the ball velocity after an impact occurs.

In general, a hybrid dynamical system can be characterized by a collection of (smooth) vector fields, event and reset functions

$$\left\{ f_{M_i} : \mathbb{R} \times \mathbb{R}^d \times \mathbb{R}^d \rightarrow \mathbb{R}^d \right\}_{i=1}^{K_M}, \quad \left\{ h_{E_j} : \mathbb{R}^d \times \mathbb{R}^d \rightarrow \mathbb{R} \right\}_{j=1}^{K_E} \quad \text{and} \quad \left\{ g_{R_m} : \mathbb{R}^d \rightarrow \mathbb{R}^d \right\}_{m=1}^{K_R},$$

respectively, with $d, K_M, K_E, K_R \in \mathbb{N}$. Here, the subindex M_i , $i = 1, \dots, K_M$, represents a mode of operation of the system, for which the system dynamics is described by the smooth vector field f_{M_i} . Each mode of operation is defined within a subregion of the state space \mathbb{R}^d . The boundaries of these subregions are determined by the zero-set of the smooth scalar functions h_{E_j} , $j = 1, \dots, K_E$. The subindex E_j represents in this case an event related to e.g. collisions, switches, etc., as outlined at the beginning of this section. Whenever a system trajectory reaches one of these boundaries, the final state of the system is mapped to the initial state of the next solution branch via a predefined reset function g_{R_m} , for some fixed

$m = 1, \dots, K_R$. A periodic solution of a hybrid dynamical system can then be represented by a sequence of *segments* $\{I_{s_n}\}_{n=1}^{K_S}$, $1 \leq s_n \leq K_I$, also referred to as *solution signature*. Here, $K_S \in \mathbb{N}$ represents the length of the signature, while $K_I \in \mathbb{N}$ stands for the total number of available segments. Each segment is associated with a vector field, an event function and a reset function, i.e. $I_\ell := \{M_{i_\ell}, E_{j_\ell}, R_{m_\ell}\}$ for all $\ell = 1, \dots, K_I$, $1 \leq i_\ell \leq K_M$, $1 \leq j_\ell \leq K_E$, $1 \leq m_\ell \leq K_R$. More details about this formulation can be found in [23, 25].

3. An impact oscillator with a time-delayed feedback controller

The physical model of the impact oscillator to be considered in the present article is shown in Fig. 3.1. The model is comprised of a mass m connected to a frame via a linear spring k_1 and a damper c . A secondary linear spring k_2 is attached to the frame at a distance g from the equilibrium position of the mass. The frame is subject to an external harmonic excitation, in such a way that when the amplitude of the mass oscillation is larger than the gap g , the mass impacts the secondary spring and hence the restoring force is governed by the overall stiffness $k_1 + k_2$. During operation, the difference $y - g$ is monitored so as to detect an impact between the mass and the secondary spring. Thus, the system can operate under one of two modes at any time: *no contact* or *contact* with the secondary spring.

3.1. Mathematical model

The nondimensional equations of motion of the impact oscillator can be written in compact form as follows [30, 31]:

$$\begin{cases} x'(\tau) = v(\tau), \\ v'(\tau) = a\omega^2 \sin(\omega\tau) - 2\zeta v(\tau) - x(\tau) - \beta(x(\tau) - e)H(x(\tau) - e), \end{cases} \quad (3.1)$$

where $H(\cdot)$ stands for the Heaviside step function and x', v' denote differentiation with respect to the nondimensional time τ . In system (3.1), the variables and parameters of the system have been nondimensionalized as follows:

$$\begin{aligned} \omega_n &= \sqrt{\frac{k_1}{m}}, & \tau &= \omega_n t, & \omega &= \frac{\Omega}{\omega_n}, & \zeta &= \frac{c}{2m\omega_n}, \\ x &= \frac{y}{y_0}, & e &= \frac{g}{y_0}, & a &= \frac{A}{y_0}, & \beta &= \frac{k_2}{k_1}, \end{aligned} \quad (3.2)$$

where $y_0 > 0$ is an arbitrary reference distance, ω_n is the natural angular frequency, ω is the frequency ratio, β is the stiffness ratio, ζ is the damping ratio, a is the nondimensionalized forcing amplitude, and e is the nondimensionalized gap.

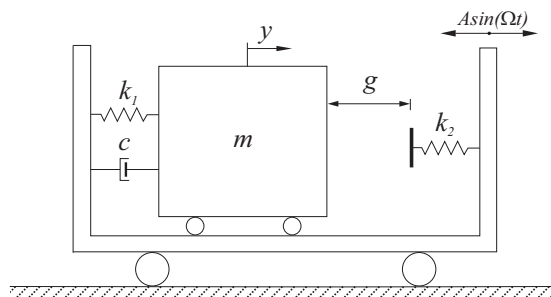


Figure 3.1: Physical model of the impact oscillator.

In the present work, we will consider a control signal $u(\tau)$, $\tau \geq 0$, which will be applied to the system's external excitation as follows

$$\begin{cases} x'(\tau) = v(\tau), \\ v'(\tau) = (a\omega^2 \sin(\omega\tau) + u(\tau)) - 2\zeta v(\tau) - x(\tau) - \beta(x(\tau) - e)H(x(\tau) - e), \end{cases} \quad (3.3)$$

where

$$u(\tau) = K (v(\tau - \tau_d) - v(\tau)), \quad \tau \geq 0, \quad (3.4)$$

defines the time-delayed feedback controller. In the expression above, $K \geq 0$ represents a control gain used to calibrate the coupling strength between the impact oscillator and the controller, while $\tau_d > 0$ stands for a predefined time delay.

3.2. Preliminary transformations

Since most of the continuation packages are written for autonomous systems, we will consider the following standard nonlinear oscillator [51] that will be appended to the equations of motion:

$$\begin{cases} r'(\tau) = r(\tau) + \omega s(\tau) - r(\tau) (r(\tau)^2 + s(\tau)^2), \\ s'(\tau) = s(\tau) - \omega r(\tau) - s(\tau) (r(\tau)^2 + s(\tau)^2), \end{cases} \quad (3.5)$$

which has the asymptotically stable solution, $r(\tau) = \sin(\omega\tau)$ and $s(\tau) = \cos(\omega\tau)$, $\tau \geq 0$. In this way, we can write the periodically forced model as an autonomous system. Furthermore, to allow the time delay $\tau_d > 0$ vary as a control parameter, it is convenient to perform a re-scaling of the model according to

$$\tilde{t} = \frac{\tau}{\tau_d}, \quad \tilde{x}(\tilde{t}) = x(\tau_d \tilde{t}), \quad \tilde{v}(\tilde{t}) = v(\tau_d \tilde{t}), \quad (3.6)$$

and hence it follows that

$$u(\tau) = u(\tau_d \tilde{t}) = K (v(\tau_d \tilde{t} - \tau_d) - v(\tau_d \tilde{t})) = K (\tilde{v}(\tilde{t} - 1) - \tilde{v}(\tilde{t})) =: \tilde{u}(\tilde{t}).$$

In this way, the numerical approximation of the resulting DDE will be carried out for a fixed delay (equal to 1), which will facilitate the time discretization, while the effective control delay τ_d can be now embedded into the system as follows (cf. (3.3), (3.5) and (3.6))

$$\begin{cases} \tilde{x}'(\tilde{t}) = \tau_d \tilde{v}(\tilde{t}), \\ \tilde{v}'(\tilde{t}) = \tau_d \left((a\omega^2 r(\tilde{t}) + \tilde{u}(\tilde{t})) - 2\zeta \tilde{v}(\tilde{t}) - \tilde{x}(\tilde{t}) - \beta(\tilde{x}(\tilde{t}) - e)H(\tilde{x}(\tilde{t}) - e) \right), \\ r'(\tilde{t}) = r(\tilde{t}) + \omega \tau_d s(\tilde{t}) - r(\tilde{t}) (r(\tilde{t})^2 + s(\tilde{t})^2), \\ s'(\tilde{t}) = s(\tilde{t}) - \omega \tau_d r(\tilde{t}) - s(\tilde{t}) (r(\tilde{t})^2 + s(\tilde{t})^2), \end{cases} \quad (3.7)$$

where now the derivatives are given with respect to the re-scaled time \tilde{t} . In what follows, all tildes will be dropped for the sake of simplicity.

3.3. Formulation of the model as a hybrid dynamical system

Let us define $\alpha := (\omega, a, \beta, \zeta, e, K, \tau_d) \in (\mathbb{R}_0^+)^7$ and $z := (x, v, r, s)^T \in \mathbb{R}^4$ as the parameters and state variables of the system, respectively, where \mathbb{R}_0^+ represents the set of nonnegative numbers. As explained in Section 2.3, the trajectories of the impact oscillator (3.7) can be divided into segments, as detailed below:

No contact (NC). This segment occurs when the mass m is not in contact with the secondary spring k_2 (see Fig. 3.1), i.e. $x - e < 0$. The dynamics of the system during this regime is governed by the

(smooth) DDE (cf. (3.7))

$$z'(t) = f_{\text{NC}}(z(t), z(t-1), \alpha) := \begin{pmatrix} \tau_d v(t) \\ \tau_d \left(a\omega^2 r(t) + K(v(t-1) - v(t)) - 2\zeta v(t) - x(t) \right) \\ r(t) + \omega\tau_d s(t) - r(t) \left(r(t)^2 + s(t)^2 \right) \\ s(t) - \omega\tau_d r(t) - s(t) \left(r(t)^2 + s(t)^2 \right) \end{pmatrix}. \quad (3.8)$$

This segment terminates when the mass hits the secondary spring k_2 , which can be detected via the condition $h_{\text{imp}}(z(t), z(t-1), \alpha) := x(t) - e = 0$. After the contact occurs, the initial point for the next segment is given by the jump function $g_{\text{id}}(z) := z$.

Contact (C). During this segment, the mass is in contact with the secondary spring (i.e. $x - e \geq 0$), and the behavior of the system is described by the equation (cf. (3.7))

$$z'(t) = f_{\text{C}}(z(t), z(t-1), \alpha) := \begin{pmatrix} \tau_d v(t) \\ \tau_d \left(a\omega^2 r(t) + K(v(t-1) - v(t)) - 2\zeta v(t) - x(t) - \beta(x(t) - e) \right) \\ r(t) + \omega\tau_d s(t) - r(t) \left(r(t)^2 + s(t)^2 \right) \\ s(t) - \omega\tau_d r(t) - s(t) \left(r(t)^2 + s(t)^2 \right) \end{pmatrix}, \quad (3.9)$$

The terminal point of this segment occurs when the mass loses contact with the secondary spring, which again can be detected via the condition $h_{\text{imp}}(z(t), z(t-1), \alpha) = 0$, as before. In this case, the initial point for the next segment is given by the jump function g_{id} previously defined.

In the mathematical framework introduced in Section 2.3, the segments defined above can be expressed as follows: $I_1 := \{\text{NC}, \text{imp}, \text{id}\}$ (*no contact*) and $I_2 := \{\text{C}, \text{imp}, \text{id}\}$ (*contact*), where the labels stand for the corresponding vector field describing the dynamics of the operation mode, the event function that defines the terminal condition and the jump function, which is in both cases just the identity function, since no impulsive phenomena are considered. Consequently, every solution to system (3.7) can be characterized by a sequence $\{I_{s_n}\}_{n=1}^{K_S}$, with $1 \leq s_n \leq 2$, which is referred to as the solution signature, as defined earlier. Under this setting, the mathematical model of the considered impact oscillator can be written in compact form as follows

$$\begin{cases} z'(t) = f_{\text{NC}}(z(t), z(t-1), \alpha), & h_{\text{imp}}(z(t), z(t-1), \alpha) < 0 \quad (\text{no contact}), \\ z'(t) = f_{\text{C}}(z(t), z(t-1), \alpha), & h_{\text{imp}}(z(t), z(t-1), \alpha) \geq 0 \quad (\text{contact}). \end{cases} \quad (3.10)$$

3.4. Finite-dimensional approximation of the model

Note that the set of DDEs (3.10) introduced in the previous section to describe the behavior of the impact oscillator can be interpreted as a piecewise-smooth dynamical system of infinite dimension. Therefore, in order to study numerically the dynamics of the system, we need first to obtain a finite-dimensional approximation of the model (3.10). For this purpose, we will employ the numerical approach described in Section 2.2 in order to obtain a piecewise-smooth system of ODEs of large dimension. Once the system of ODEs has been constructed, it can then be solved numerically by any standard integration technique [52], including path-following methods for piecewise-smooth systems, as will be done here.

Let us consider the state variable $\tilde{z} := (x, r, s, u_0, \dots, u_N, w_1, \dots, w_N)^T \in \mathbb{R}^{2N+4}$. Hence, by applying

the numerical approximation given by (2.7) to (3.8), we obtain the system of ODEs

$$\begin{aligned} \tilde{z}'(t) &= \tilde{f}_{\text{NC}}(\tilde{z}(t), \alpha) \\ &:= \begin{pmatrix} \tau_d u_0(t) \\ r(t) + \omega \tau_d s(t) - r(t) (r(t)^2 + s(t)^2) \\ s(t) - \omega \tau_d r(t) - s(t) (r(t)^2 + s(t)^2) \\ \tau_d \left(a \omega^2 r(t) + K (u_N(t) - u_0(t)) - 2\zeta u_0(t) - x(t) \right) \\ (w_i(t))_{i=1, \dots, N} \\ \left(2N^2 \left(u_{i-1}(t) - u_i(t) - \frac{1}{N} w_i(t) \right) \right)_{i=1, \dots, N} \end{pmatrix}, \end{aligned} \quad (3.11)$$

which gives a finite-dimensional approximation of the DDE (3.8), corresponding to the *no contact* mode. Here, we are assuming that $u_0(t) = v(t)$ and

$$u_i(t) \approx v(t - t_i), \quad \text{for all } t \geq 0, \quad t_i = \frac{i}{N}, \quad i = 1, \dots, N. \quad (3.12)$$

Note that owing to the transformation (3.6), the time discretization is carried out over the unit interval, regardless the value of the delay τ_d . Following the same procedure, we obtain another set of ODEs for the *contact* regime

$$\begin{aligned} \tilde{z}'(t) &= \tilde{f}_{\text{C}}(\tilde{z}(t), \alpha) \\ &:= \begin{pmatrix} \tau_d u_0(t) \\ r(t) + \omega \tau_d s(t) - r(t) (r(t)^2 + s(t)^2) \\ s(t) - \omega \tau_d r(t) - s(t) (r(t)^2 + s(t)^2) \\ \tau_d \left(a \omega^2 r(t) + K (u_N(t) - u_0(t)) - 2\zeta u_0(t) - x(t) - \beta(x(t) - e) \right) \\ (w_i(t))_{i=1, \dots, N} \\ \left(2N^2 \left(u_{i-1}(t) - u_i(t) - \frac{1}{N} w_i(t) \right) \right)_{i=1, \dots, N} \end{pmatrix}, \end{aligned} \quad (3.13)$$

In this way, the original infinite-dimensional, piecewise-smooth system (3.10) can be approximated by the following system of finite dimension

$$\begin{cases} \tilde{z}'(t) = \tilde{f}_{\text{NC}}(\tilde{z}(t), \alpha), & x(t) - e < 0 \quad (\text{no contact}), \\ \tilde{z}'(t) = \tilde{f}_{\text{C}}(\tilde{z}(t), \alpha), & x(t) - e \geq 0 \quad (\text{contact}). \end{cases} \quad (3.14)$$

With this mathematical setup we are ready to test the proposed numerical approach to approximate the solution of piecewise-smooth DDEs.

4. Numerical investigation of the dynamical response of the controlled impact oscillator

4.1. Preliminary numerical studies

Our preliminary analysis of the impact oscillator (3.1) begins with the multistable scenario where two stable attractors coexist. Fig. 4.1 shows the bifurcation of the system without the delayed feedback control when its stiffness ratio varies in the range $\beta \in [20, 100]$. As can be seen from the figure, blue dots represent a period-2 attractor with two impacts, and red dots denote a period-2 attractor with one impact. The impact oscillator is monostable exhibiting the period-2 motion with one impact for $\beta \in [20, 27.081)$, and when $\beta \approx 27.081$, the period-2 motion with two impacts emerges. As can be seen from the right windows of Fig. 4.1, the period-2 motion with two impacts becomes more stable as the stiffness ratio increases, and the basin of the period-2 motion with one impact shrinks. Next, we will apply the delayed

feedback controller and investigate the dynamics of the impact oscillator under variation of the control parameter K .

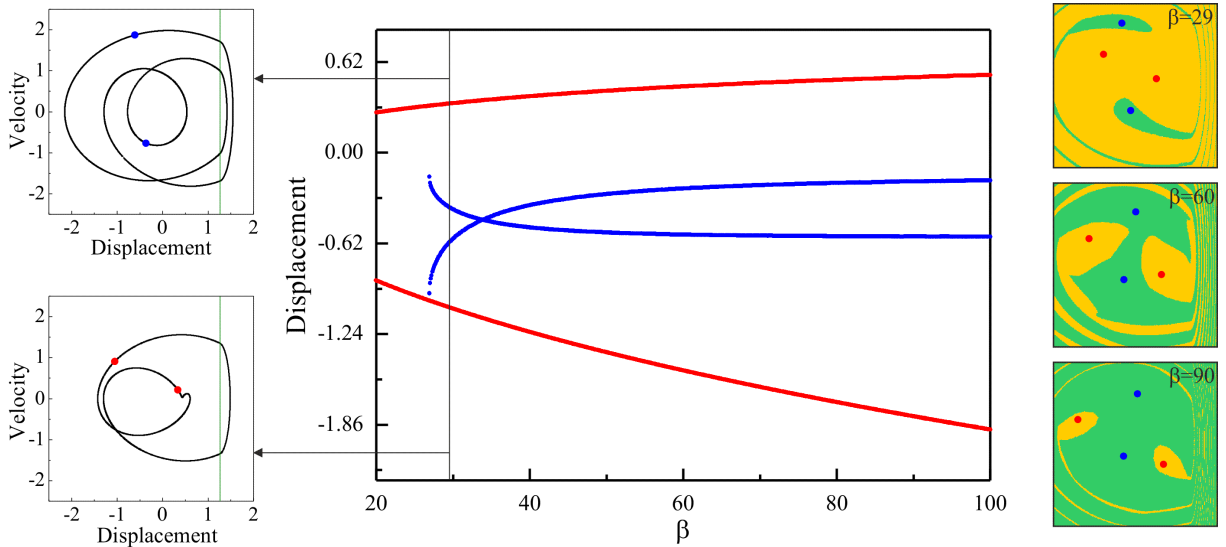


Figure 4.1: (Colour online) Bifurcation diagram of the impact oscillator without the delayed feedback controller computed for $\omega = 0.8$, $a = 0.9$, $\zeta = 0.01$, $e = 1.26$ by varying the stiffness ratio β . Blue dots represent the period-2 attractor with two impacts per period of excitation, red dots denote the period-2 attractor with one impact per period of excitation. The location of the impact boundary is shown by the vertical green line. Right windows show the evolution of basins of attraction of the system as the stiffness ratio increases.

Bifurcation diagram for the controlled impact oscillator under variation of the control parameter K is presented in Fig. 4.2. As the control parameter increases up to $K \approx 0.0027$, the period-2 attractor with two impacts disappears and the system becomes monostable. A comparison of this bistability with and without the delayed feedback controller is shown in the left windows of Fig. 4.2, where the basin for the period-2 attractor with two impacts shrinks as the control parameter K increases. Thereafter, only the period-2 attractor with one impact exists until a reverse period doubling encountered at $K = 0.177$, and the system bifurcates into a period-1 motion with one impact per period of excitation. Examples of the impact oscillator controlled from bistable to monostable is given in Fig. 4.3, where time histories of the external excitation (including the delayed feedback control) and the displacement of the impact oscillator are presented. As can be seen from the figure, the controller was switched on at $\tau = 4000$, and both the period-2 attractor with two impacts and the period-2 attractor with one impact were controlled to a new period-2 attractor with one impact per period of excitation.

4.2. Numerical tests of the approximation scheme for piecewise-smooth DDEs

In Section 3.4 we introduced a piecewise-smooth ODE of large dimension approximating the original DDE model (3.10). This approximation was based on the numerical scheme explained in detail in Section 2.2, where the main idea is to introduce auxiliary functions defined via suitable time shifts of the exact solution, which are then expanded through a Taylor series of a predefined order. The time shift is defined, after re-scaling (see (3.6)), over the unit interval, at the grid points $t_i = \frac{i}{N}$, $i = 0, \dots, N$, with $N \in \mathbb{N}$ sufficiently large. This allows us to obtain a finite-dimensional approximation of a DDE, which then can be solved numerically by any standard integration technique. In this section we will investigate numerically the approximation properties of the piecewise-smooth ODE (3.14) introduced in Section 3.4, as the dimension of this system varies with the discretization parameter N .

In Fig. 4.4 we present a numerical comparison of the dynamical behavior of the original piecewise-smooth DDE (3.10) with the approximating system of ODEs (3.14), for different values of the delay parameter τ_d . In this diagram, and in the remainder of this work, all DDE and ODE models are

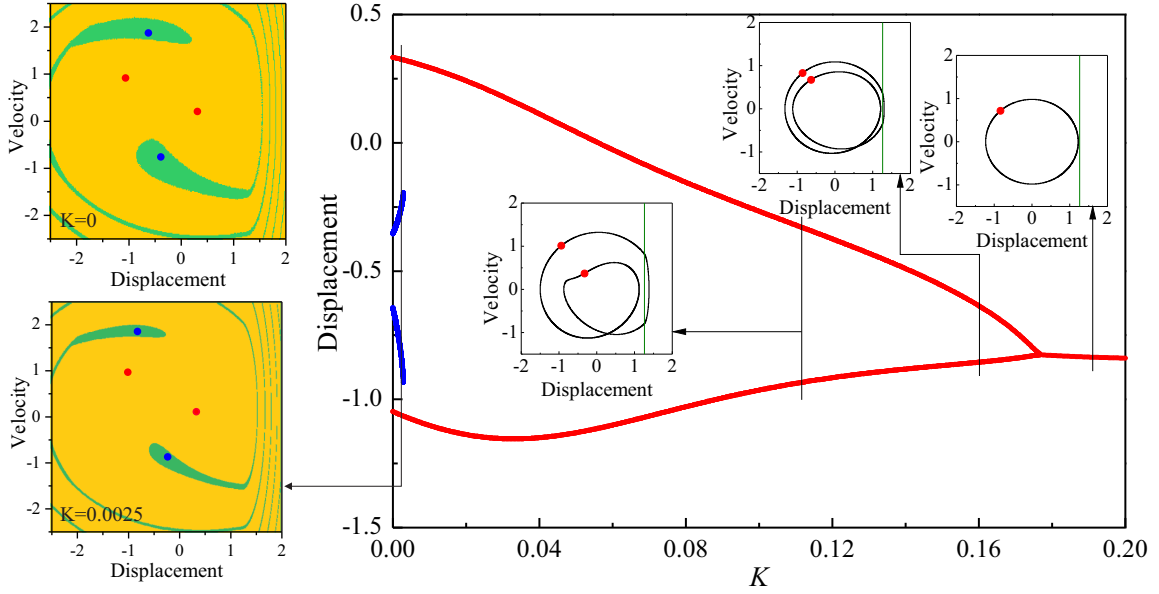


Figure 4.2: (Colour online) Bifurcation diagram of the impact oscillator with the delayed feedback controller computed for $\omega = 0.8$, $a = 0.9$, $\zeta = 0.01$, $e = 1.26$, $\beta = 29$, $\tau_d = 3.8$ by varying the control parameter K . Red dots represent the period-2 attractor with one impact, and blue dots denote the period-2 attractor with two impacts per period of excitation. Left windows compare the basins of attraction of the system with ($K = 0.0025$) and without ($K = 0$) the time-delayed feedback controller.

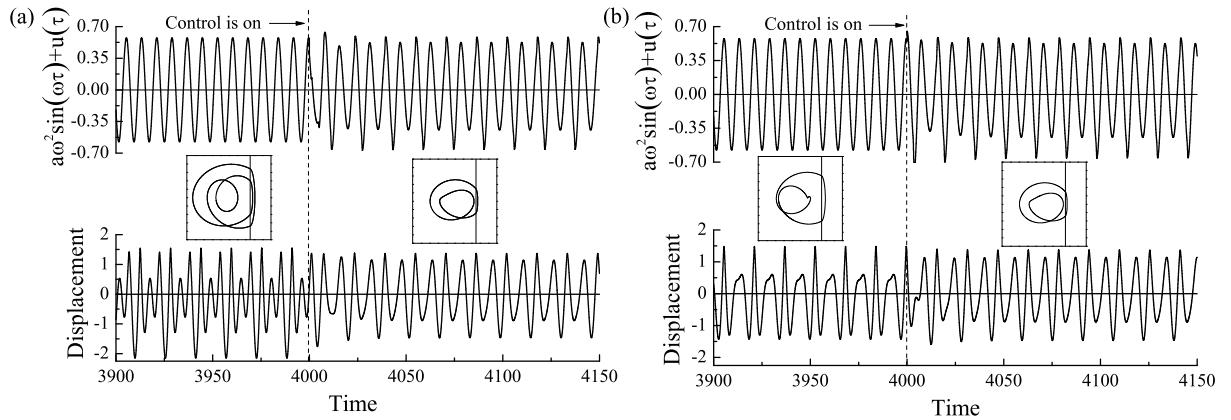


Figure 4.3: Trajectories and external excitations of the impact oscillator with the delayed feedback controller, computed for $\omega = 0.8$, $a = 0.9$, $\zeta = 0.01$, $e = 1.26$, $\beta = 29$, $K = 0.12$ and $\tau_d = 3.8$. The impact oscillator is controlled from (a) the period-2 attractor with two impacts and (b) the period-2 attractor with one impact to a new period-2 attractor with one impact per period of excitation.

integrated using the MATLAB solvers ‘dde23’ and ‘ode15s’, respectively, in combination with their built-in event location routines [53, 54] so as to detect accurately collisions with the impact boundary $x = e$. For the chosen discretization parameter $N = 50$ (which gives a step-size $\frac{1}{N} = 0.02$), we can observe that the computed solutions of the original DDE (plotted in red, dashed lines) and the approximating ODE system (blue, solid lines) are very close to each other, for different values of τ_d . In addition, for each case the figure presents time plots showing trajectories for $u_0(t)$ ($= v(t)$, in blue) and $u_N(t)$ ($\approx v(t - 1)$, in black), corresponding to the solutions of the approximating system (3.14) (see (3.12)). From these plots we can observe that the proposed numerical scheme provides reasonable approximations of the original

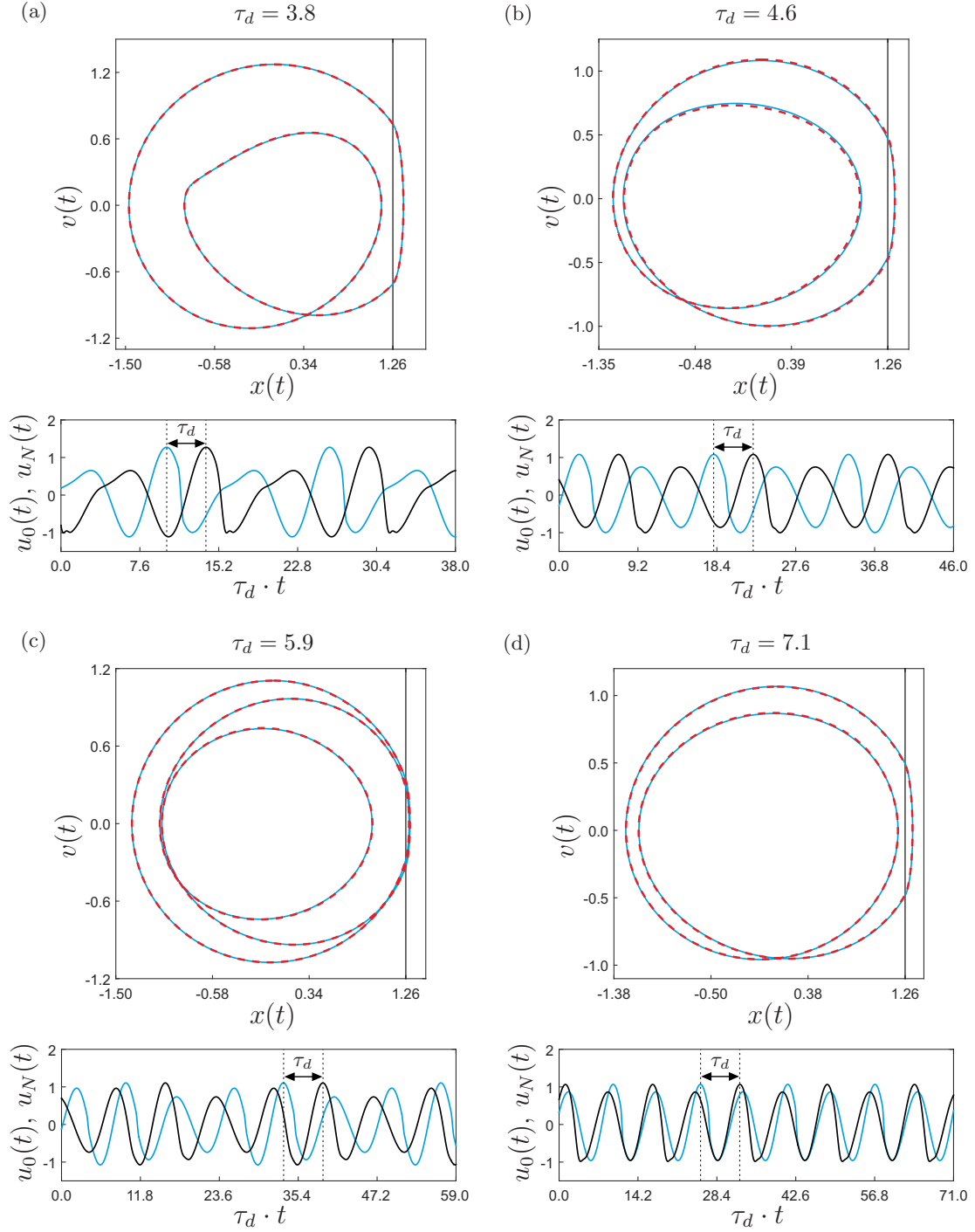


Figure 4.4: Numerical comparison of the dynamical response of the piecewise-smooth DDE (3.10) with the approximating system of ODEs (3.14), for the parameter values $\omega = 0.8$, $a = 0.9$, $\zeta = 0.01$, $e = 1.26$, $\beta = 29$, $K = 0.12$ and $N = 50$. Panels (a) to (d) show phase plots for $\tau_d = 3.8$, $\tau_d = 4.6$, $\tau_d = 5.9$ and $\tau_d = 7.1$, respectively. The solutions to the original system (3.10) and their approximations are depicted in red (dashed line) and in blue (solid line), respectively. In all phase plots, the vertical black line stands for the impact boundary $x = e$. The time plots show the behavior of $u_0(t)$ ($= v(t)$, in blue) and $u_N(t)$ ($\approx v(t-1)$, in black), corresponding to the solutions of the approximating system (3.14) (see (3.12)). The time plots are given with respect to the original timescale $\tau_d \cdot t$, see (3.6).

DDE, although the time plots present some perturbations of the solution observable in the lower peaks, produced by a well-known effect referred to as *numerical distortion*, which typically appears in semi-discretization schemes as the one proposed in the present work [55]. This numerical distortion, however, does not affect significantly the approximation of the orbits depicted in the phase plots shown in Fig. 4.4.

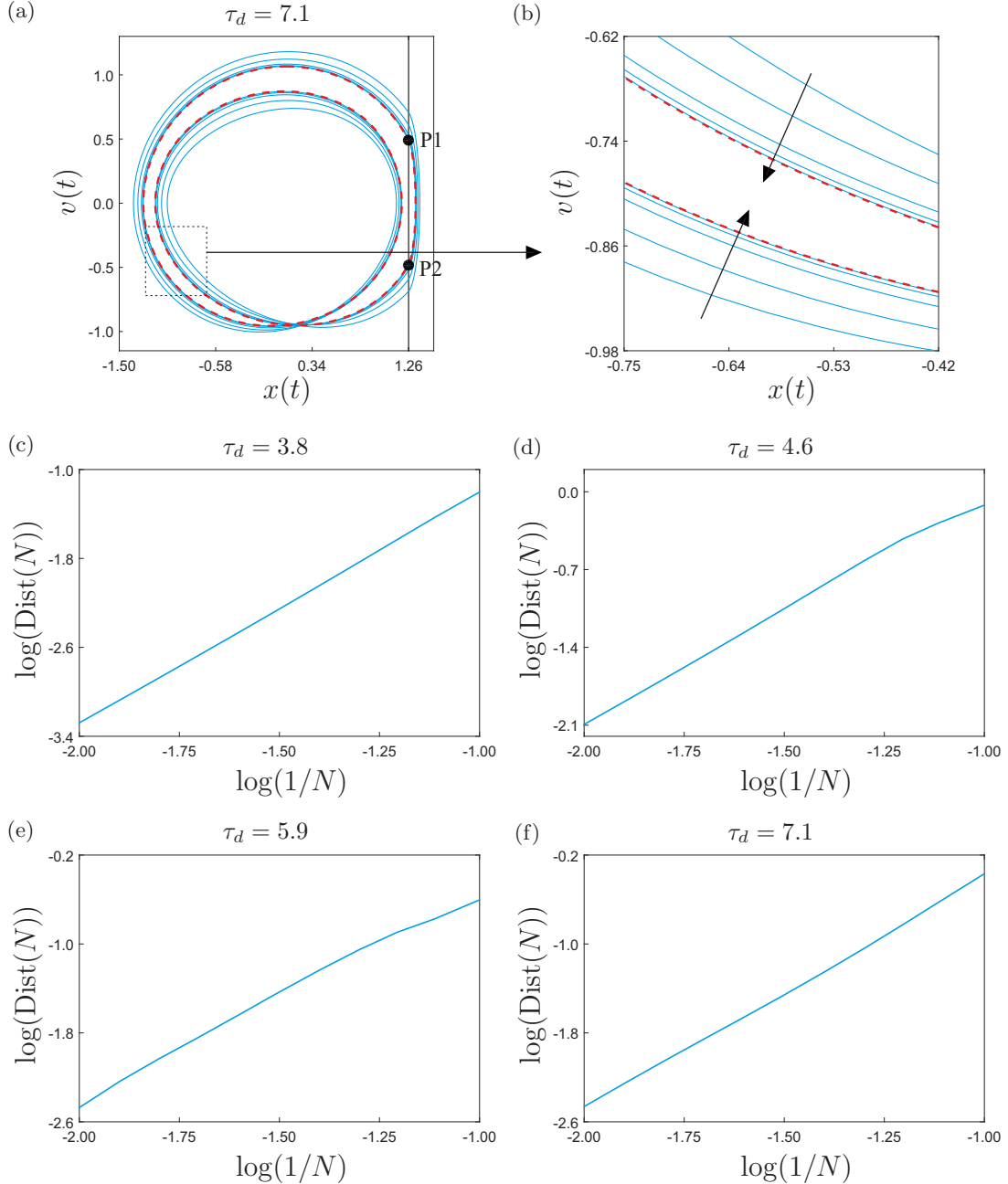


Figure 4.5: (a) Family of approximating orbits (in blue) computed from the system of ODEs (3.14), for the parameter values used in Fig. 4.4 (with $\tau_d = 7.1$) and $10 \leq N \leq 100$. Here, the reference solution of the piecewise-smooth DDE (3.10) is plotted in red (dashed line), showing the intersections P1 and P2 with the discontinuity boundary $x = e$. An enlargement of the boxed region is depicted in panel (b), where the arrows indicate the direction of increasing N . Panels (c) to (f) show the behavior of the distance function (4.1) as N varies, computed for $\tau_d = 3.8$, $\tau_d = 4.6$, $\tau_d = 5.9$ and $\tau_d = 7.1$, respectively, using the reference solutions (in red, dashed lines) depicted in Fig. 4.4.

Next, we will investigate numerically some of the convergence properties of the proposed numerical

scheme to approximate the solution of piecewise-smooth DDEs. Specifically, we will focus on the experimental order of approximation for the specific case of the impact oscillator driven by a time-delayed feedback controller, considered in the present work. For this purpose, we will define a suitable distance function that will allow us to quantify how close a solution of the original DDE and its numerical approximation are, as the step-size $\frac{1}{N}$ varies. This study is also motivated by the fact that local truncation errors act as perturbations to the original system whose solutions are approximated, and in some cases the computed solutions may exhibit high sensitivity when the mesh width is varied [56].

To investigate the approximation properties of the proposed numerical scheme, let us consider bounded periodic solutions of the piecewise-smooth DDE (3.10), and assume that the solutions intersect (transversally) the impact boundary ($x = e$) $m \geq 2$ times, at the points $(x_1, v_1), \dots, (x_m, v_m)$, with $(x_i, v_i) \in \mathbb{R}^2$, for $i = 1, \dots, m$. Let us pick one of such solutions and consider the corresponding numerical approximation computed from the piecewise-smooth system of ODEs (3.14). If N is sufficiently large, then the approximating solution will also intersect the impact boundary m times, at the points $(\tilde{x}_1^{(N)}, \tilde{v}_1^{(N)}), \dots, (\tilde{x}_m^{(N)}, \tilde{v}_m^{(N)})$. Assuming a suitable ordering of the intersection points, we define the distance function

$$\text{Dist}(N) := \sum_{i=1}^m \left\| (x_i, v_i) - (\tilde{x}_i^{(N)}, \tilde{v}_i^{(N)}) \right\|, \quad (4.1)$$

where $\|\cdot\|$ stands for the Euclidean norm in \mathbb{R}^2 . This function can be used as a quantitative indicator of how close a solution of the original DDE and its numerical approximation are, when the step-size $\frac{1}{N}$ is adjusted.

The main results are shown in Fig. 4.5. Panel (a) presents a periodic solution of the original piecewise-smooth DDE (3.10) (plotted in red, dashed lines) together with a family of approximating solutions computed from the system of ODEs (3.14) (in blue), with $10 \leq N \leq 100$ and $\tau_d = 7.1$. In this picture, it can be observed that the approximating solutions indeed become closer and closer to the reference solution as the mesh width $\frac{1}{N}$ decreases. This procedure was repeated also for $\tau_d = 3.8$, $\tau_d = 4.6$ and $\tau_d = 5.9$, and the convergence was verified as well. A closer look into the convergence is obtained from panels (c) to (f), where the behavior of the distance function defined in (4.1) is analyzed with respect to variations of N , on a logarithmic scale, for the values of τ_d considered above. The panels reveal an almost linear response indicating that the distance function decreases according to $\mathcal{O}(N^{-p})$, with $p \approx 2$. This observed order of accuracy is consistent with the second-order approximation given by (2.7) and applied in (3.14), which confirms the reliability of the proposed numerical scheme to approximate the solution of piecewise-smooth DDEs. In what follows and unless otherwise indicated, we will use $N = 15$ in our numerical study, which was found to be a suitable value to keep a good balance between computational cost and accuracy of the results.

4.3. Numerical investigation of the time-delayed impact oscillator via continuation methods

In this section, our main purpose will be the application of the proposed numerical approach to study the dynamics of the considered impact oscillator with time-delayed feedback control, via continuation techniques. The starting point for this numerical investigation will be the periodic solution computed in Fig. 4.4(a) (the one in blue, computed from system (3.14)). To begin with, let us take first the control delay τ_d as the bifurcation parameter and investigate how the initial periodic solution behaves as this parameter is changed. The result is presented in Fig. 4.6. The figure includes a diagram showing the behavior of the test function

$$h_{\text{GR}}(z(t), \alpha) := x(t) - e, \quad (4.2)$$

which is evaluated at a suitably chosen point along a periodic solution where the mass velocity is zero (for example at the point Pt shown in one of the phase plots in Fig. 4.6). In this way, an accurate detection of grazing events is possible. As can be observed in the figure, the bifurcation diagram is limited by two grazing bifurcations, labeled GR1 and GR2, detected at $\tau_d \approx 3.1903$ and $\tau_d \approx 4.6563$, respectively, whose phase plots are depicted in the smaller external panels. A closer look to the system dynamics around the grazing point GR2 reveals a period-doubling effect produced when the grazing contact occurs, when

GR2 is crossed from above, which is a classical phenomenon observed near grazing points, see e.g. [50, Section 6.3.3].

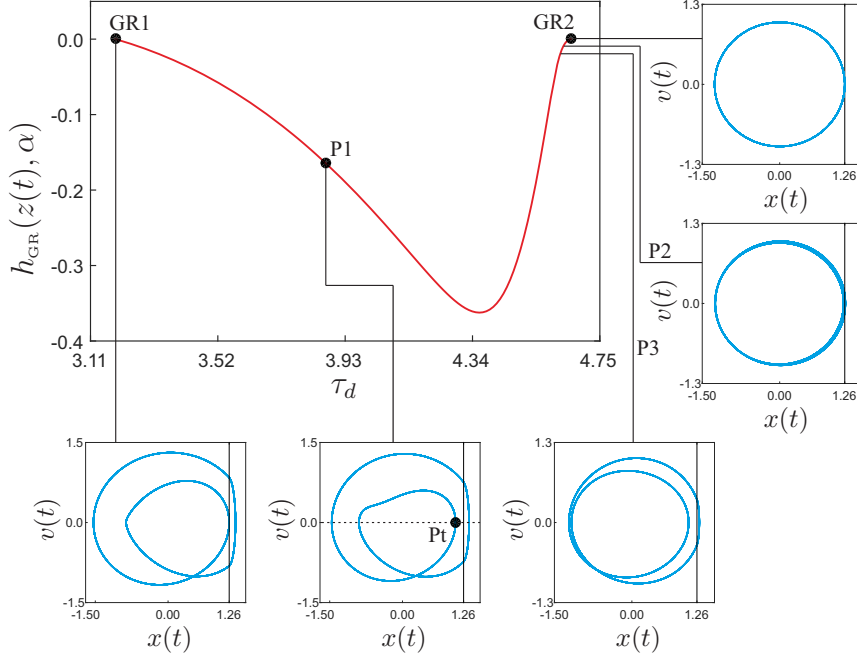


Figure 4.6: Continuation of the periodic response of system (3.14) with respect to the control delay τ_d , for the parameter values given in Fig. 4.4. The diagram presents the behavior of the test function h_{GR} introduced in (4.2) to detect grazing events. The labels GR1 and GR2 stand for grazing bifurcations detected at $\tau_d \approx 3.1903$ and $\tau_d \approx 4.6563$, respectively. The phase plots show periodic solutions computed at GR1, GR2 and at the test points P1 ($\tau_d = 3.868$), P2 ($\tau_d = 4.620$) and P3 ($\tau_d = 4.558$).

Next, let us investigate the periodic response of the approximating system (3.14) as the control gain K is varied. The result of this study is presented in Fig. 4.7, where the plot shows the contact time, i.e., the time the mass is in contact with the secondary spring within one orbital period, as a function of K . As can be seen in this diagram, large values of K induce a periodic response with no impacts with the secondary spring, hence the contact time equals zero. As this parameter decreases, a periodic solution with a tangential intersection with the impact boundary $x = e$ is detected at the point labeled GR, found for $K \approx 0.1747$. Therefore, this value defines a boundary between impacting and non-impacting periodic behavior. In addition, further investigations reveal that this grazing bifurcation also produces a period-doubling effect, similarly to the case studied in the previous paragraph. The bifurcation diagram finishes at $K = 0$, corresponding to the situation when the time-delayed feedback controller is switched off, due to which any delay effect disappears from the model. In this case the original DDE model (3.10) and its approximating system of ODEs (3.14) are equivalent.

As can be observed from the studies above, the dynamics of the controlled impact oscillator is dominated by the presence of grazing phenomena. In particular, our investigation revealed that the time-delayed feedback controller is able to drive the system from impacting to non-impacting responses and viceversa, where the boundary point is defined by a grazing bifurcation. Therefore, we will next carry out a two-parameter continuation of this critical point with respect to the main control parameters, i.e., the control delay τ_d and the control gain K . The result of this process is displayed in Fig. 4.8. Panel (a) shows a curve representing all combinations of τ_d and K producing periodic solutions making tangential contact with the impact boundary $x = e$. In this way, the parameter space is divided locally by this curve into two regions. The first one (above the curve) corresponds to all pairs (τ_d, K) for which the system presents non-impacting periodic solutions, as the one computed at the test point P2 (see panel (d)). On the contrary, below the grazing curve, we find operation points (τ_d, K) producing impacting periodic solutions, for instance at the test points P1 and P3, depicted in panels (c) and (e), respectively.

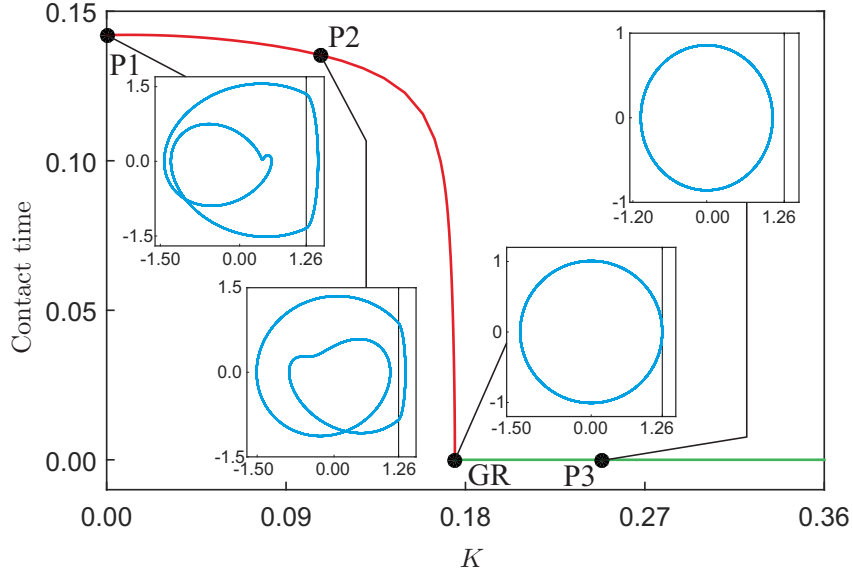


Figure 4.7: Continuation of the periodic response of system (3.14) with respect to the control gain K , for the parameter values given in Fig. 4.4, with $\tau_d = 3.8$. The diagram presents the time spent during the *contact* mode (see Section 3.3) on the vertical axis. The label GR represents a grazing bifurcation found at $K \approx 0.1747$. The inner panels show phase plots on the x - v plane for the test points P1 ($K = 0$), P2 ($K = 0.1071$), P3 ($K = 0.2482$) and GR.

In panels (c) to (e), the solutions to the original system (3.10) and their approximations (computed from system (3.14)) are depicted in red (dashed line) and in blue (solid line), respectively. Furthermore, in Fig. 4.8(b) we plot the solution manifold computed along the grazing curve displayed in panel (a), showing the components $u_0(t) (= v(t))$, $u_N(t) (\approx v(t - 1))$ and the delay parameter τ_d . In this graph, two particular values can be identified. The first one, when τ_d takes the value closest to zero, we can observe that the phase plot corresponding to this value resembles the identity function. This is because, since the delay is close to zero, both the signals $v(\tau)$ and $v(\tau - \tau_d)$ (in the original time scale) are almost in phase, and this is reflected on the phase plane u_0 - u_N . A similar phenomenon can be observed for $\tau_d = 2\pi/\omega \approx 3.927$, where the signals are 180 degrees out phase, which can also be identified from the 3D plot.

5. Concluding Remarks

Piecewise-smooth dynamical systems with delay have been widely used in the past to describe complex phenomena in a variety of research areas, for instance in biology, mechanics and control. Despite the popularity and importance of such type of models, the available computational tools for numerical study and simulation are rather limited, owing to the infinite-dimensional nature of dynamical systems with delay, in combination with the analytical and numerical difficulties arising when nonsmooth phenomena are considered. While a number of software packages have been developed for numerical continuation in smooth DDEs (e.g. DDE-BIFTOOL [10], PDDE-CONT [12] and Knut [13]), no software package of this kind exists for the path-following analysis of piecewise-smooth DDEs. There is, however, a solid computational framework developed for this purpose (see for instance [28]), but the related codes are not yet available in a user friendly form.

The present work proposed a numerical approach for the numerical continuation of periodic solutions of nonsmooth dynamical systems with delay. The numerical approach is based on the well-known technique of approximating delay differential equations via large systems of ODEs. Such approximating systems were developed and studied since mid 1960s, see for example the works by Krasovskii [45], Repin [14] and Westdal [16]. In particular, it has been shown that the solution of the approximating systems of ODEs converges uniformly to the solution of the original DDE as the number of ODEs tends to infinity [14]. Further results regarding convergence have been derived thereafter, see for instance the studies by

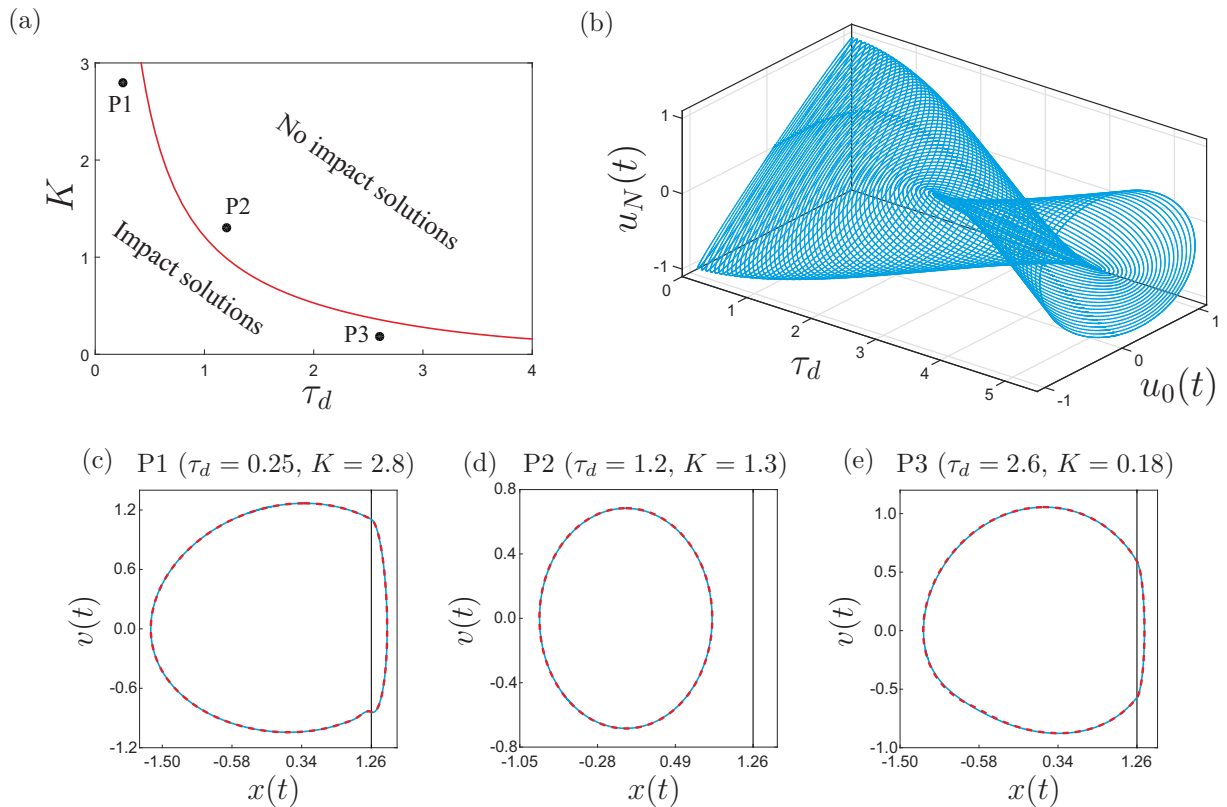


Figure 4.8: (a) Continuation in two parameters of the grazing bifurcation (GR) encountered in Fig. 4.7, with respect to τ_d and K . The resulting curve defines the boundary between impacting and non-impacting responses. (b) Solution manifold computed along the grazing curve plotted in (a). The axes show the components $u_0(t)$ ($= v(t)$), $u_N(t)$ ($\approx v(t-1)$) and the delay parameter τ_d . Panels (c) to (e) show phase plots computed at the test points P1, P2 and P3, respectively, marked in panel (a). The solutions to the original system (3.10) and their approximations (computed from system (3.14)) are depicted in red (dashed line) and in blue (solid line), respectively.

Gyori et al. [15, 46], Banks [18] and Demidenko [47], as well as recent applications in practical problems [19, 48]. Following these previous works, in the present study we applied a second-order approximation of the original DDE by considering a finite sequence of Taylor expansions as proposed in [29]. In this way, a piecewise-smooth dynamical system with (constant) delay can be approximated by a piecewise-smooth system of ODEs of large dimension, which then allows the study of the resulting model in the framework of hybrid dynamical systems, following the ideas of [28] and [23]. This enables the numerical bifurcation study of the system response via path-following methods, for instance via the general-purpose continuation platform COCO [25].

The effectiveness of the proposed scheme was tested on a well-known and widely studied impact oscillator [30, 31], driven by a time-delayed feedback controller. One of the advantages of the proposed numerical approach is that it allows the study of discontinuity-induced bifurcations, such as sliding and grazing, a task that is difficult to perform if discontinuity boundaries are not clearly identified in the numerical implementation, for instance when smoothing the original system via e.g. parameter-dependent families of tanh functions. Via the numerical software COCO, we carried out the numerical continuation of periodic solutions of the impact oscillator, with special focus on detection of grazing phenomena when the main control parameters are varied, specifically, the control delay τ_d and the control gain K . Our investigation revealed that the considered time-delayed feedback controller is able to steer the system from impacting to non-impacting responses and viceversa, where the boundary point is defined by a grazing bifurcation. By using the COCO capability of tracing loci of special points in two parameters, we carried out the two-parameter continuation of the detected grazing bifurcation with respect to τ_d and K . In this way, we obtained a curve in the τ_d - K plane defining the boundary between impacting and

non-impacting periodic behavior.

Although the proposed numerical approach provides a straightforward mean to study piecewise-smooth dynamical systems with delay via existing and well-established continuation packages, it suffers from a number of limitations. To begin with, a significant increase of computation time can be noticed when the mesh width $\frac{1}{N}$ decreases (see (2.7)), which is an unavoidable effect owing to the infinite-dimensional nature of dynamical systems with delay. Nevertheless, our numerical investigation showed that still a good balance between computational cost and accuracy of the results can be found. It is also important to mention that in our implementation we have not tracked secondary discontinuities that are known to be propagated as the time increases. Due to the well-known *smoothing* property of DDEs [39], this does not seem to affect the numerical accuracy in the considered continuation framework (since our study focused on periodic solutions), however, this is something that needs to be looked into when dealing with DDEs with nonsmooth phenomena. Therefore, in the long term future work should focus on the development of general-purpose, portable and user friendly computational tools for the numerical continuation and bifurcation analysis of piecewise-smooth dynamical systems with delay, combining the capabilities offered by e.g. DDE-BIFTOOL and the multi-segment continuation toolbox of COCO.

Acknowledgements

This work has been supported by EPSRC under Grant No. EP/P023983/1, and was partially supported by the National Natural Science Foundation of China (Grant No. 11672257). Mr. Zhi Zhang would like to acknowledge the financial support from the University of Exeter for his Exeter International Excellence Scholarship. Finally, the authors would like to express their gratitude to Prof. Jan Sieber (Exeter University) for helpful remarks on this work.

References

- [1] L. C. Davis, “Modifications of the optimal velocity traffic model to include delay due to driver reaction time,” *Physica A*, vol. 319, pp. 557–567, 2003.
- [2] L. E. Kollar, G. Stepan, and J. Turi, “Dynamics of delayed piecewise linear systems,” in *Proceedings of the 5th Mississippi State Conference on Differential Equations and Computational Simulations*, (Mississippi, USA), pp. 163–185, 2003.
- [3] V. Kapila, W. M. Haddad, and A. Apostolos, “Stabilization of linear systems with simultaneous state, actuation, and measurement delays,” *Int. J. Control*, vol. 72, no. 18, pp. 1619–1629, 1999.
- [4] J. Nilsson, B. Bernhardsson, and B. Wittenmark, “Stochastic analysis and control of real-time systems with random time delays,” *Automatica*, vol. 34, no. 1, pp. 57–64, 1998.
- [5] F. S. Borges, K. C. Iarosz, H. P. Ren, A. M. Batista, M. S. Baptista, R. L. Viana, S. R. Lopes, and C. Grebogi, “Model for tumour growth with treatment by continuous and pulsed chemotherapy,” *BioSystems*, vol. 116, no. 1, pp. 43–48, 2014.
- [6] A. R. M. Carvalho and C. M. A. Pinto, “New developments on AIDS-related cancers: The role of the delay and treatment options,” *Math. Meth. Appl. Sci.*, pp. 1–14, 2017. Article in press.
- [7] K. Nandakumar and M. Wiercigroch, “Stability analysis of a state dependent delayed, coupled two DOF model of drill-string vibration,” *J. Sound Vibration*, vol. 332, no. 10, pp. 2575–2592, 2013.
- [8] T. Zhang, X. Meng, and Y. Song, “The dynamics of a high-dimensional delayed pest management model with impulsive pesticide input and harvesting prey at different fixed moments,” *Nonlinear Dynamics*, vol. 64, no. 1-2, pp. 1–12, 2011.
- [9] K. Pyragas, “Continuous control of chaos by self-controlling feedback,” *Phys. Lett. A*, vol. 170, no. 6, pp. 421–428, 1992.

- [10] K. Engelborghs, T. Luzyanina, and D. Roose, “Numerical bifurcation analysis of delay differential equations using DDE-BIFTOOL,” *ACM Trans. Math. Software*, vol. 28, no. 1, pp. 1–21, 2002.
- [11] J. Sieber, K. Engelborghs, T. Luzyanina, G. Samaey, and D. Roose, “DDE-BIFTOOL Manual—Bifurcation analysis of delay differential equations.” Available at <http://sourceforge.net/projects/ddebiftool>, 2017.
- [12] R. Szalai, G. Stépán, and S. J. Hogan, “Continuation of bifurcations in periodic delay-differential equations using characteristic matrices,” *SIAM J. Sci. Comput.*, vol. 28, no. 4, pp. 1301–1317, 2006.
- [13] R. Szalai, “Knut: A continuation and bifurcation software for delay-differential equations.” Available at <http://rs1909.github.io/knut>. Department of Engineering Mathematics, University of Bristol, United Kingdom, 2013.
- [14] I. M. Repin, “On the approximate replacement of systems with lag by ordinary dynamical systems,” *J. Appl. Math. Mech.*, vol. 29, no. 2, pp. 254–264, 1965.
- [15] I. Györi and J. Turi, “Uniform approximation of a nonlinear delay equation on infinite intervals,” *Nonlinear Analysis*, vol. 17, no. 1, pp. 21–29, 1991.
- [16] J. A. Westdal and W. H. Lehn, “Time optimal control of linear systems with delay,” *Int. J. Control*, vol. 11, no. 4, pp. 599–610, 1970.
- [17] R. A. Hess, “Optimal control approximations for time delay systems,” *AIAA Journal*, vol. 10, no. 11, pp. 1536–1538, 1972.
- [18] H. T. Banks, “Approximation of nonlinear functional differential equation control systems,” *J. Optim. Theory Appl.*, vol. 29, no. 3, pp. 383–408, 1979.
- [19] G. Lipták, K. M. Hangos, and G. Szederkényi, “Approximation of delayed chemical reaction networks,” *React. Kinet. Mech. Catal.*, vol. 123, no. 2, pp. 403–419, 2018.
- [20] S. H. Doole and S. J. Hogan, “A piecewise linear suspension bridge model: Nonlinear dynamics and orbit continuation,” *Dynam. Syst.*, vol. 11, no. 1, pp. 19–45, 1996.
- [21] E. Fossas, “Study of chaos in the buck converter,” *IEEE Trans. Circuits Syst. I*, vol. 43, no. 1, pp. 13–25, 1996.
- [22] P. Piironen, *Recurrent dynamics of nonsmooth systems with application to human gait*. PhD thesis, KTH Royal Institute of Technology, Sweden, 2002.
- [23] P. Thota and H. Dankowicz, “TC-HAT: A Novel Toolbox for the Continuation of Periodic Trajectories in Hybrid Dynamical Systems,” *SIAM J. Appl. Dyn. Sys.*, vol. 7, no. 4, pp. 1283–1322, 2008.
- [24] F. Dercole and Y. A. Kuznetsov, “SlideCont: An Auto97 Driver for Bifurcation Analysis of Filippov Systems,” *ACM Trans. Math. Software*, vol. 31, no. 1, pp. 95–119, 2005.
- [25] H. Dankowicz and F. Schilder, *Recipes for continuation*. Computational Science and Engineering, Philadelphia: SIAM, 2013.
- [26] D. A. W. Barton, B. Krauskopf, and R. E. Wilson, “Explicit periodic solutions in a model of a relay controller with delay and forcing,” *Nonlinearity*, vol. 18, no. 6, pp. 2637–2656, 2005.
- [27] D. A. W. Barton, B. Krauskopf, and R. E. Wilson, “Periodic solutions and their bifurcations in a non-smooth second-order delay differential equation,” *Dynam. Syst.*, vol. 21, no. 3, pp. 289–311, 2006.
- [28] D. A. W. Barton, “Stability calculations for piecewise-smooth delay equations,” *Internat. J. of Bif. and Chaos*, vol. 19, no. 2, pp. 639–650, 2009.

- [29] W. Weckesser, “VFGEN: A code generation tool,” *J. Numer. Anal. Ind. Appl. Math.*, vol. 3, no. 1-2, pp. 151–165, 2008.
- [30] J. Ing, E. E. Pavlovskaja, M. Wiercigroch, and S. Banerjee, “Experimental study of impact oscillator with one-sided elastic constraint,” *Philos. Trans. R. Soc. Lond., Ser. A, Math. Phys. Eng. Sci.*, vol. 366, no. 1866, pp. 679–704, 2008.
- [31] S. Banerjee, J. Ing, E. E. Pavlovskaja, M. Wiercigroch, and R. Reddy, “Invisible grazings and dangerous bifurcations in impacting systems: The problem of narrow-band chaos,” *Physical Review E*, vol. 79, no. 3, 2009.
- [32] E. Allgower and K. Georg, *Introduction to Numerical Continuation Methods*, vol. 45 of *Classics in Applied Mathematics*. New York: SIAM, 2003.
- [33] E. J. Doedel, A. R. Champneys, T. F. Fairgrieve, Y. A. Kuznetsov, B. Sandstede, and X.-J. Wang, *Auto97: Continuation and bifurcation software for ordinary differential equations (with HomCont)*. Computer Science, Concordia University, Montreal, Canada, 1997. Available at <http://cmvl.cs.concordia.ca>.
- [34] Y. A. Kuznetsov and V. V. Levitin, “CONTENT: A multiplatform environment for analyzing dynamical systems.” Available at <http://www.math.uu.nl/people/kuznet/CONTENT/>. Dynamical Systems Laboratory, Centrum voor Wiskunde en Informatica, Amsterdam, 1997.
- [35] A. Dhooge, W. Govaerts, and Y. A. Kuznetsov, “MATCONT: A MATLAB package for numerical bifurcation analysis of ODEs,” *ACM Trans. Math. Software*, vol. 29, no. 2, pp. 141–164, 2003.
- [36] S. Guo and J. Wu, *Bifurcation theory of functional differential equations*, vol. 184 of *Applied Mathematical Sciences*. New York: Springer-Verlag, 2013.
- [37] O. Diekmann, S. A. van Gils, S. M. Verduyn Lunel, and H.-O. Walther, *Delay equations*, vol. 110 of *Applied Mathematical Sciences*. New York: Springer-Verlag, 1995.
- [38] M. Lakshmanan and D. V. Senthilkumar, *Dynamics of nonlinear time-delay systems*. Springer Series in Synergetics, New York: Springer-Verlag, 2010.
- [39] J. K. Hale and S. M. Verduyn Lunel, *Introduction to functional differential equations*, vol. 99 of *Applied Mathematical Sciences*. New York: Springer-Verlag, 1993.
- [40] Y. Kuang, *Delay differential equations*, vol. 191 of *Mathematics in Science and Engineering*. Boston: Academic Press, 1993.
- [41] L. E. El’sgol’ts and S. B. Norkin, *Introduction to the theory and application of differential equations with deviating arguments*, vol. 372 of *Mathematics in Science and Engineering*. New York: Academic Press, 1973.
- [42] H. T. Banks, “Delay systems in biological models: Approximation techniques,” in *Nonlinear Systems and Applications* (V. Lakshmikantham, ed.), pp. 21–38, London: Academic Press, 1977.
- [43] A. Stefanski, A. Dabrowski, and T. Kapitaniak, “Evaluation of the largest Lyapunov exponent in dynamical systems with time delay,” *Chaos, Solitons and Fractals*, vol. 23, no. 5, pp. 1651–1659, 2005.
- [44] T. Kapitaniak, “Chaotic behaviour of anharmonic oscillators with time delay,” *J. Phys. Soc. Jpn.*, vol. 56, no. 6, pp. 1951–1954, 1987.
- [45] N. N. Krasovskii, “The approximation of a problem of analytic design of controls in a system with time-lag,” *J. Appl. Math. Mech.*, vol. 28, no. 4, pp. 876–885, 1964.
- [46] B. Krasznai, I. Gyori, and M. Pituk, “The modified chain method for a class of delay differential equations arising in neural networks,” *Math. Comput. Model.*, vol. 51, no. 5-6, pp. 452–460, 2010.

- [47] G. V. Demidenko and V. A. Likhoshvai, “On differential equations with retarded argument,” *Sib. Math. J.*, vol. 46, no. 3, pp. 417–430, 2005.
- [48] M. Gomoyunov and A. Plaksin, “Finite-dimensional approximations of neutral-type conflict-controlled systems,” *IFAC-PapersOnLine*, vol. 50, no. 1, pp. 5109–5114, 2017.
- [49] M. Benchohra, J. Henderson, and S. Ntouyas, *Impulsive Differential Equations and Inclusions*, vol. 2 of *Contemporary Mathematics and Its Applications*. New York: Hindawi Publishing Corporation, 2006.
- [50] M. di Bernardo, C. J. Budd, A. R. Champneys, and P. Kowalczyk, *Piecewise-smooth dynamical systems. Theory and Applications*, vol. 163 of *Applied Mathematical Sciences*. New York: Springer-Verlag, 2004.
- [51] B. Krauskopf, H. Osinga, and J. Galán-Vioque, eds., *Numerical Continuation Methods for Dynamical Systems*. Understanding Complex Systems, Netherlands: Springer-Verlag, 2007.
- [52] E. Hairer, S. P. Nørsett, and G. Wanner, *Solving Ordinary Differential Equations I*. New York: Springer-Verlag, second ed., 1993.
- [53] L. F. Shampine and S. Thompson, “Event location for ordinary differential equations,” *Comput. Math. Appl.*, vol. 39, no. 5-6, pp. 43–54, 2000.
- [54] L. F. Shampine and S. Thompson, “Solving DDEs in MATLAB,” *Appl. Numer. Math.*, vol. 37, no. 4, pp. 441–458, 2001.
- [55] A. Vande Wouwer, P. Saucez, and W. Schiesser, eds., *Adaptive method of lines*. New York: Chapman & Hall, 2001.
- [56] R. J. LeVeque, *Finite difference methods for ordinary and partial differential equations*. Philadelphia: SIAM, 2007.